EUROPEAN FUSION DEVELOPMENT AGREEMENT
JET

EFDA–JET–CP(02)03/09

R.Barnsley, I.Coffey, R.Lucock, and M.F.Stamp

JET Beam-Line with Integrated X-Ray VUV and Visible Spectrometers, for Burning Plasma Experiments

JET Beam-Line with Integrated X-Ray VUV and Visible Spectrometers, for Burning Plasma Experiments

R.Barnsley[1], I.Coffey[1], R.Lucock, M.F.Stamp
and contributors to the EFDA-JET workprogramme*

[1]*Department of Pure and Applied Physics, Queens University Belfast, BT7 1NN, UK*
** See annex of J. Pamela et al, "Overview of Recent JET Results and Future Perspectives", Fusion Energy 2000 (Proc. 18th International Conference on Controlled Fusion and Plasma Physics, Sorrento, 2000), IAEA, Vienna (2001)*

Pre-Print of paper to be submitted for publication in proceedings of the 17th Topical Conference on High Temperature Plasma Diagnostics, Madison, USA, 08 - 11 July, 2002

ABSTRACT

We report several developments to the JET Tokamak survey spectroscopy beamline, which now supports a suite of X-ray, VUV and visible instruments, located in a radiation-shielded bunker outside the torus hall. The instruments have vacuum systems that are integrated into the tritium circuit, and are available for D-T experiments. The x-ray and VUV diagnostics have real-time data reduction. The proposed plasma impurity monitor for ITER is based on these developments.

1. INTRODUCTION

Spectroscopic monitoring of the plasma impurities will be essential for a burning plasma experiment such as ITER. A spectroscopic diagnostic system must be tritium compatible, and be shielded against neutron and gamma radiation. A wide spectral coverage, ranging from the visible to x-rays, is necessary in order to maximise the number of observed ions and ionisation stages. For plasmas with burn-times of hundreds of seconds, real-time data reduction will be essential for machine protection.

The vacuum spectroscopy beamline no JET has been incrementally upgraded to incorporate the above requirements, all of which have been demonstrated. Originally the beamline, with its shielded bunker outside the JET torus hall (fig.1), was dedicated to a two-reflection x-ray crystal spectrometer [1]. This instrument had excellent shielding, but a rather modest time resolution and spectral coverage. Experience during JET D-T experiments [2] showed that a single reflection crystal spectrometer [3] could have shielding adequate for any future D-T experiments on JET, while having much improved sensitivity, time-resolution and spectral coverage.

Until recently, the VUV (10 – 100nm) and XUV (1 – 40nm) grating spectrometers were located in the torus hall, close-coupled to JET. They were not operated during D-T experiments because they had no shielding, and their vacuum systems were not compatible with tritium. Even during high-power D-D discharges, the neutron and gamma ray induced background was appreciable. The VUV spectrometer has been moved outside the torus hall, sharing the vacuum beam-line via a mirror, and giving a large improvement in shielding and accessibility. A visible sight line has also been included, primarily as a window-free reference channel for visible spectroscopy.

2. INTEGRATION OF SPECTROMETERS ONTO SHIELDED BEAMLINE

The x-ray, VUV and visible spectrometers share the beamline via mirror a chamber (fig.2) which divides the available aperture with suitably angled mirrors, with the x-ray beam passing through undeflected.

The main reason for the mirror before the VUV spectrometer is to collimate the beam, matching the beamline divergence of ~1/200 to spectrometer divergence of ~1/50. A valuable consequence is the offset of the grating and detector from the direct line of sight, thereby further improving the shielding. The mirror was designed with the aid of the in-house OPTIC [3] ray-tracing code, with parameters of the beamline and candidate mirrors being listed in Table.1. The spectrometer slit to mirror distance was dictated by available space in the bunker, a distance of just over ne metre being the most practical. A greater separation would have been more favourable, by offsetting the spectrometer further from the direct line of sight, and by reducing the magnification of the slit image at the port, the mirror grazing angle of 15° was a trade-off between space and short wavelength cut-off. Angles as low as 5° were ray-traced, and while they all wed higher reflectance from the mirror, there was insufficient clearance in the bunker. Different mirror materials were investigated, the most practical being gold, whose reflectance cut-off at 15° grazing angle (fig.3) closely matches the wavelength range of the spectrometer. Although a toroidal mirror is usually the natural choice for grazing incidence optics, ray-tracing showed that, due to the large aperture at the torus port, a spherical mirror suffices in this case. With an aperture-filling factor of 0.915, and typical mirror reflectance of 0.50, the sensitivity is reduced to 0.46 of the close-coupled value. A similar study was conducted for the XUV spectrometer, using a 5º grazing incidence nickel mirror, but this has not yet been implemented, and the instrument remains in the torus hall.

The mirror, of gold-coated glass, is mounted to a manually adjustable tilt and rotation stage. Alignment was achieved by removing the spectrometer grating and slit, and directing a H_e-N_e laser through the spectrometer centre-line, from the mirror and onto the valve at the torus-end of the beam-line. Then the slit was replaced, with a tungsten lamp behind it, to confirm that the image of the slit was focused onto the valve. The spectrometers and mirror chamber are mounted together on a rigid frame which, after alignment, was bolted to the bunker foundation. In operation, the sensitivity of the spectrometer was as predicted, and no further adjustments of the alignment have been necessary.

The mirror chamber also contains two plane mirror, one of which is coupled to a visible spectrometer via a telescope and optical fibre. Both mirrors are mounted to piezo-electric tilt stages that can be remotely adjusted while the system is under vacuum. The mirror for the visible channel is of aluminised glass with a MgF_2 protective coating, and an incident angle of 45°. Alignment was initially achieved by shining a laser down the fibre and adjusting the mirror angles and telescope focus until the fibre image was fully contained on the torus valve, as seen by a telescope via the spare mirror. Subsequently, with the torus valve open, the location of the spot no the torus inner-wall was confirmed by the JET In-Vessel Inspection System (IVIS). The remaining mirror was designed to be suitable for a future normal-incidence VUV spectrometer, making the spectral coverage of the beamline continuous from ~0.1 nm to ~1000 nm.

The vacuum system is tritium-compatible, and exhausts to the JET tritium circuit. Ingress of tritium is minimised by a secondary beamline gate-valve inside the bunker, in front of the mirror chamber, which is opened only during a discharge. This, combined with rapid pump-out of the system, results in minimal tritium retention. After venting, tritium levels have been measured to be low enough for maintenance to proceed without any special precautions.

2.1. VUV SPECTROMETER

The VUV spectrometer has a toroidal grating of major radius 919 mm and incident angle 70.6°, with a 450 l/mm grating normally used, covering the spectrum 10 -100 nm. The detector is a micro-channel electron multiplier with phosphor, coupled via a fibre-optic expander to a 2048 element photo-diode array. Spectra are stored every 11ms for post-pulse analysis. Specified line intensities are derived in real-time, with a delay less than 1ms, and are output digitally to the JET Real-Time Central Controller (RTCC). The Real-Time Signal Server (RTSS) makes signals available for further processing or for feed-back control. Real-time line intensities for Fe XXIII and Ni XXV are shown in fig.4, compared with post-pulse values. The Fe XXIII signal is interlocked to the operation of lower hybrid current drive, in order to protect the launcher.

Mirror grazing angle (deg.)	Slit-mirror distance (mm)	Mirror-port distance (mm)	Port Height (mm)	Port Width (mm)	Typical mirror reflectance, 10-100nm
15	1138	18200	165.5	101.3	0.50

Mirror Type	R1 (mm)	R2 (mm)	Height of slit image at port (mm)	Width of slit image at port (mm)	Fraction of image within existing port
Plane	-	-	190	500	0.172
Spherical (selected)	**8276**	**-**	**180**	**8**	**0.915**
Toroidal	8276	554	36	8	1.0
Ellipsoidal	-	-	36	1	1.0

TABLE 1: Parameter of candidate mirror, obtained with the OPTIC ray-tracing code. A toroidal mirror gives a better focus, but a spherical mirror is adequate for the large port at the torus. Including the mirror reflectance, the sensitivity is effectively 0.46 of the close-coupled value.

Relocating the instrument outside the torus hall, in addition to giving improved reliability and easier access, has resulted in a large improvement in the signal-to-noise ratio. Figure 5 shows the noise levels in the VUV “SPRED” and XUV “SOXMOS ” spectrometers during D-D neutron production, comparing the background away from any spectral lines, with the neutron rate, RNT. With both instruments in the torus hall, time evolution of the background closely matches the neutron rate. With the VUV spectrometer moved outside the torus hall, its background carries little or no signature of the neutron rate, with at least an order of magnitude improvement in the signal-to-noise ratio. Figure 6 shows spectra from the same discharges as shown in fig.5, where inside the torus hall, even for D-D discharges, the neutron-induced noise level exceeds that of many weaker lines. With the instrument outside the torus hall, the background during the peak neutron production at 7.6s is almost identical to that during the pre-neutron phase at 5.4s. This improved shielding, coupled with the tritium compatible vacuum system, makes the instrument available for future D-T experiments on JET. Because the beamline apertures, both at the bunker and torus ends, are much larger than required to enclose the optical path from mirror to torus, the neutron and gamma ray flux at the spectrometer is about 100 times higher than it would be with optimised shielding. It follows that the signal-to-noise performance of this system is relevant to a burning plasma.

2.2. X-RAY SPECTROMETER

The soft x-ray spectrometer [4]uses crystals and multilayer mirrors to survey the spectrum from ~0.1 nm to ~10nm, with resolving power $\lambda/\delta\lambda$ between 20 and 500, depending on the diffractor and the collimation. The flat diffractors are scanned by stepper motors, with counts from gas proportional counters being correlated with rotary encoder signals to obtain the spectra. Real-time line intensities are derived with a time resolution of about 50ms, this being mainly limited by the scanning mechanism rather than count-rate or computation. A spectrum of Be IV from the longest-wavelength channel is shown in fig.7, where the line-width is dominated by the broad diffraction peak of the Ni-C multilayer, and the slope in the continuum is due to the transmission of the 1.5 μ aluminised Mylar detector window. Measurements with different filters and detector gases, and a masked background channel, have shown that the background beneath the line is almost entirely due to diffracted continuum, even during high-power D-T discharges. Due to the low resolving power, the continuum level is relatively high, frequently exceeding the line peak. This makes it essential to measure the continuum level away from the line, so that both continuum and line intensity can be measured independently. Monitors that are fixed on the line peak give a signal which is the sum of line and continuum, and which is impossible to interpret. Examples of the real-time output of line and continuum intensities, compared with post-pulse processing, are shown in fig.8 for Be IV and O VIII. For a period of up to a year, during the preparation, execution and clean-up of JET D-T experiment [5], when the VUV and XUV instruments were taken out of operation, the soft x-ray spectrometer was the main monitor of core impurities. Fig.9 shows line and continuum intensities for the main light impurities, plotted with the neutron rate for a high-power D-T discharge. There is no signature of the neutron rate no any of the signals. The peak count-rate in the background channel was a few kHz, compared with a few MHz in the main lines, a signal-to-noise performance that is adequate for any future D-T plasmas at JET. As with the VUV spectrometer, there is scope to improve the signal-to-noise ratio by matching the beamline geometry to that of the spectrometer optics, here by about a factor 10.

2.3. VISIBLE SPECTROMETER

Figure 10 compares spectra between the close-coupled and remote visible channels, where the sensitivity of the remote view is broadly similar to the close-coupled view. The reduction of aperture incurred by the long beamline is offset by the use of much shorter optical fibres, reducing the attenuation at short wavelengths. The main motivation for including this sight line was to have a visible view with no plasma-facing window, to allow cross calibration of the close-coupled visible bremsstrahlung Z_{eff} monitors. The first optical element on the remote view is effectively the mirror, which is 20m back from the plasma, making it relatively immune from darkening by redeposition. This sight line was only recently commissioned, and no long-term data are yet available. Another use planned for this view is a branching-ratio cross-calibration from visible to VUV using the common sight line. This is expected to remove any systematic error due to variations in the local emission flower ionisation stages, which can occur with different lines of sight.

3. APPLICATIONS

In addition to advancing the survey spectroscopy on JET, developments to this beamline have been kept relevant to future burning plasma experiments such as ITER, and have been incorporated into its evolving design [6-11].

ACKNOWLEDGEMENTS

This work has been conducted under the European Fusion Development Agreement and is partly funded by Euratom and the UK Department of Trade and Industry

REFERENCES

[1]. R.Barnsley, U.Schumacher, E.Kallne, H.W.Morsi, G.Rupprecht. Double crystal spectroscopy at JET. Rev Sci Instrum, vol.62(4) April 1991, 889-898.

[2]. R.Barnsley et al, Bragg Spectroscopy of impurities during the JET preliminary tritium experiment. Rev Sci Instrum, vol63(10)Oct 1992, 5023-5025.

[3]. P.Nielsen, EFDA/ENEA Padova, Italy.

[4]. R.Barnsley, K.D.Evans, N.J.Peacock, N.C.Hawkes. Bragg rotor spectrometer for Tokamak diagnostic. Rev. Sci. Instrum. 57(8) Aug. 1986(2159)

[5]. M.Keilhacker et al, and the JET Team. High fusion performance from deuterium-tritium plasma in JET. Nucl. Fusion (1999).

[6]. R.Barnsley, R Giannella, MStamp, P Thomas. Visible grating VUV/XUV and crystal spectroscopy on ITER. ITER-IL-PH-7-0-80. Publ.by IAEA, Vienna, July 1990.

[7]. R.Barnsley, R Giannella, K D Lawson, N J Peacock. Applications of x-ray spectroscopy to ITER. “Diagnostics for experimental thermonuclear fusion reactors”, Ed.Stott et al. Plenum Press, New York (1996).

[8]. N.J.Peacock et al, Spectroscopy for impurity control on ITER. “Diagnostics for experimental thermonuclear fusion reactors”, Ed. Stott et al. Plenum Press, New York (1996).

[9]. R.Barnsley, P.H.Edmonds, R.MGiannella, M.G.O’Mullane. X-ray spectrometry system for ITER. “Diagnostics for experimental thermonuclear fusion reactors 2”, Ed. Stott et al.Plenum Press, New York (1998).

[10]. P.H.Edmonds, R.Barnsley, N.Hawkes, A.Kislyakov, G.Vayakis, C.Walker et al. Integration of vacuum coupled diagnostics (to ITER). Ibid. p79.

[11]. N.C.Hawkesetal, XUV and VUV spectroscopy of ITER. “Diagnostics for experimental thermonuclear fusion reactors 2", Ed.Stott et al. Plenum Press, New York (1998).

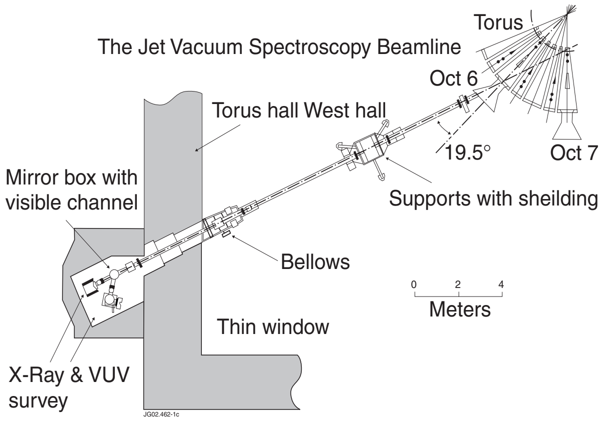

Figure 1: Three diagnostics share a shielded bunker outside the JET torus hall: a soft x-ray survey spectrometer, a VUV spectrometer, and a visible spectrometer. There is no window at the torus, and the entire beamline vacuum system is included in the JET tritium circuit.

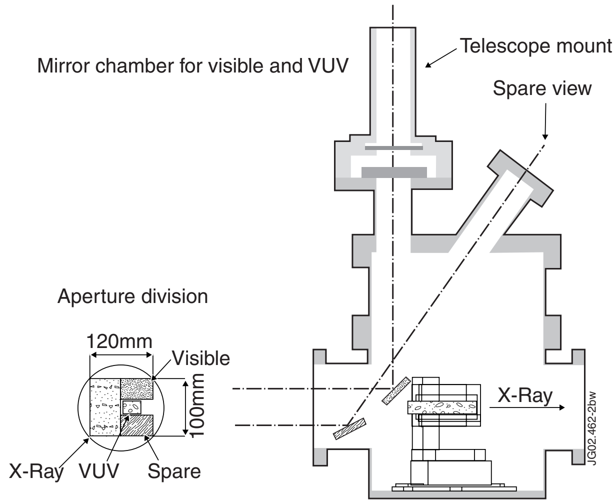

Figure 2: Mirror chamber divides the available aperture between the instruments. The x-ray path is direct, the visible channels are reflected in the vertical plane, and the VUV channel is reflected horizontally by a 15° grazing incidence spherical gold mirror.

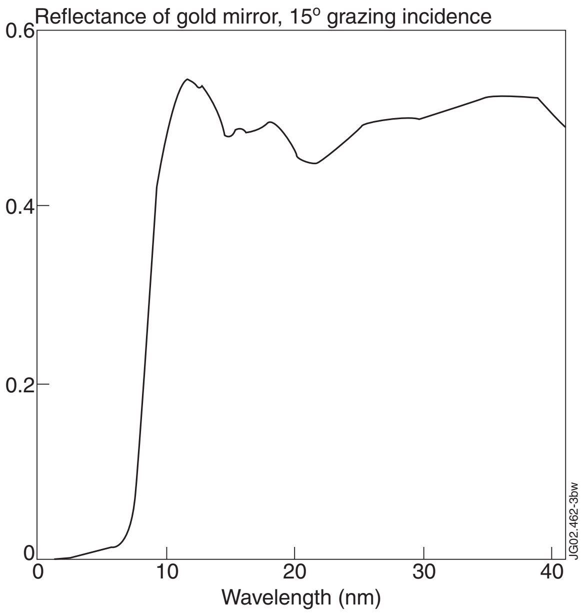

Figure 3: Reflectance of gold at 15° grazing incidence. The cutoff at below 10nm is well matched to that of the VUV spectrometer.

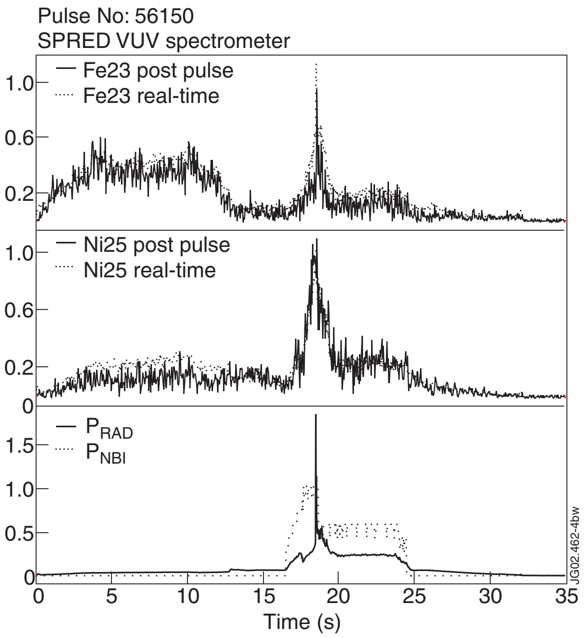

Figure 4: Real-time Fe XXIII and Ni XXV signal from the VUV spectrometer, compared with post-pulse values. The time resolution is 11ms, with a delay of about 2ms. To prevent damage to the Lower Hybrid Current Drive launcher, operation of LHCD is interlocked to the RT FE XXIII signal.

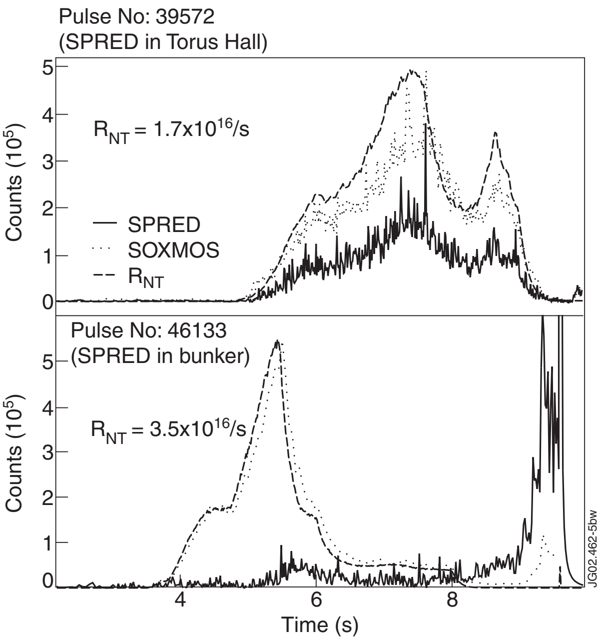

Figure 5: Noise levels in the VUV "SPRED" and XUV "SOXMOS" spectrometers during D-D neutron production, comparing the background (away from any spectral lines), with the neutron rate, R_{NT}. Top: With both instruments in the torus hall, the background closely matches the neutron rate. Bottom: With the VUV spectrometer moved outside the torus hall, viewing the plasma via a mirror, its background carries little or no signature of the neutron rate.

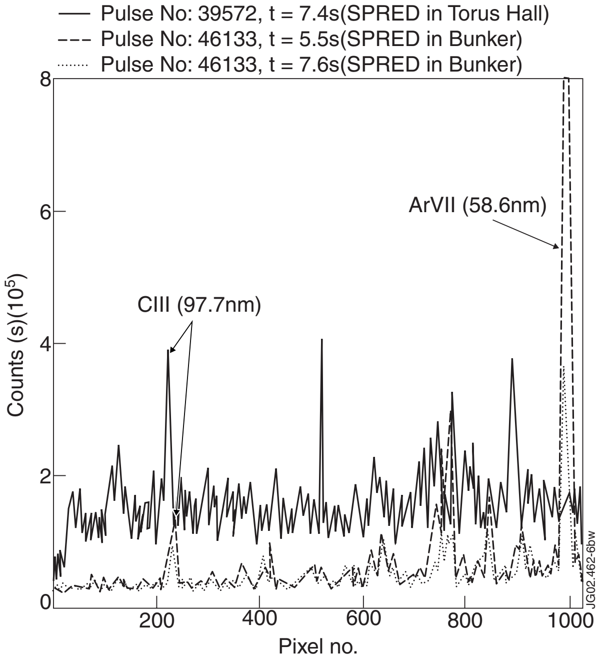

Figure 6: Spectra from the VUV spectrometer before and after its relocation from the torus hall to a shielded bunker, for the same discharges as shown in Fig.5. Inside the torus hall, the neutron-induced noise level exceeds that of many weaker lines. With the instrument outside the torus hall, the background during the peak neutron production at 7.6s is almost identical to that during the pre-neutron phase at 5.4s.

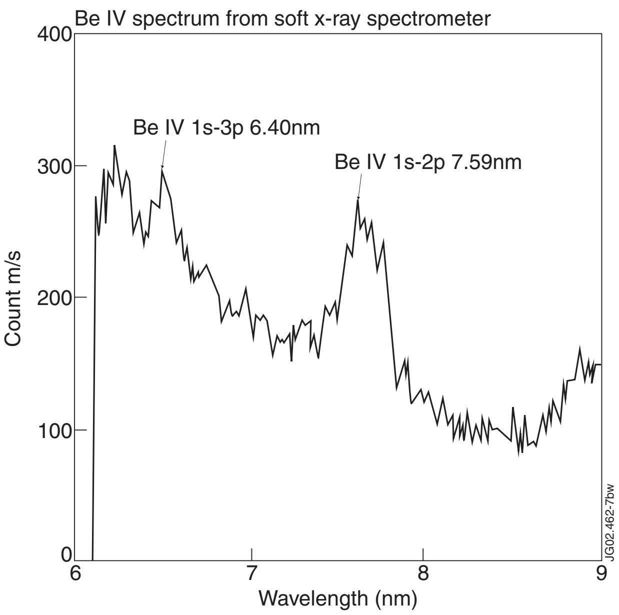

Figure 7: Typical spectrum from Channel 1 (Ni-C multilayer) of the four-channel soft x-ray survey spectrometer - a scanning monochromator. Detector and rotary encoder counts are correlated in real time, and the line and continuum intensities derived with a delay of about 20ms. The data in Fig. 10 were obtained using a narrower scan range (about 7.0-8.2nm) to improve time resolution.

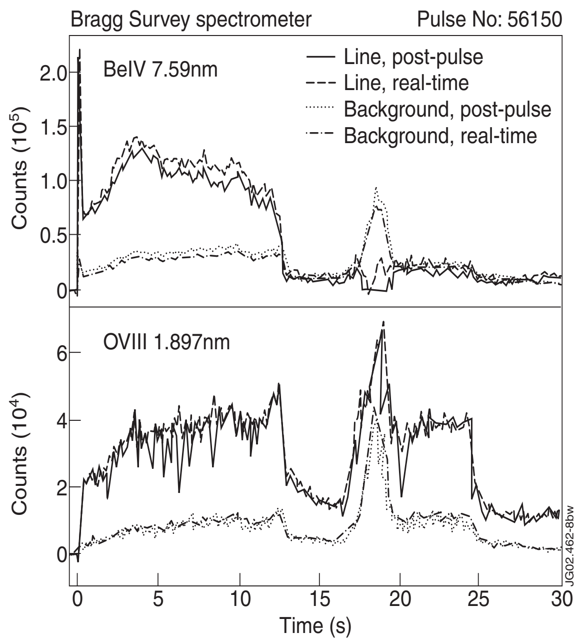

Figure 8: Real-time signals from the x-ray survey spectrometer, showing line intensities and associated continuum background for Be VI and O VIII. Most intrinsic and injected impurities can be monitored.

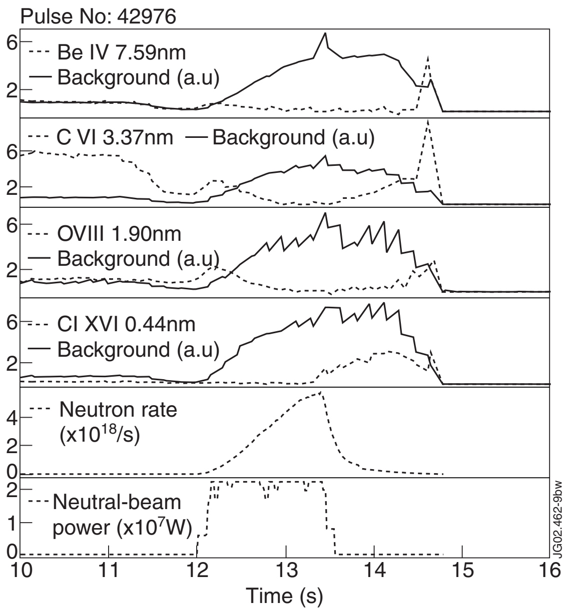

Figure 9: Line and background intensities for light impurities, from the soft x-ray survey spectrometer, during a JET high-power D-T discharge. Neither the line intensities nor the continuum background, on which the lines are sitting, show any signature of the neutron rate.

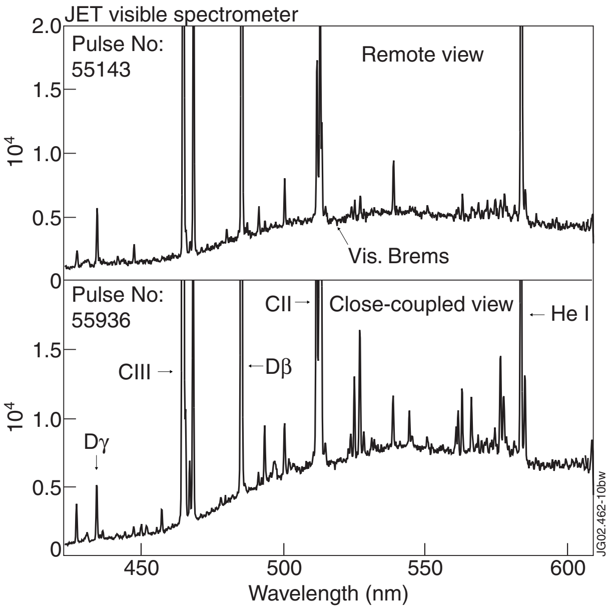

Figure 10: Comparison spectra of the remote and close-coupled visible channels. The remote view has a smaller geometrical aperture, which is partly offset by the much shorter optical fibers, leading to less fall-off at short wavelengths.